Applied Mathematics and Mechanics
(English Edition, Vol. 14, No. 6, Jun. 1993)

Published by SUT,
Shanghai, China

HARTEN SOLUTION FOR ONE-DIMENSIONAL UNSTEADY EQUATION

Chen Shao-jun (陈少军)

(Shanghai University of Technology, Shanghai)

(Received April 2, 1992; Communicated by Pan Li-zhou)

Abstract

In order to use the second-order 5-point difference scheme mentioned to compute the solution of one dimension unsteady equations of the direct reflection of the strong plane detonation wave meeting a solid wall barrier, in this paper, we technically construct the difference schemes of the boundary and sub-boundary of the problem, and deduce the auto-analogue analytic solutions of the initial value problem, and at the same time, we present a method for the singular property of the initial value problem, from which we can get a satisfactory computation result of this difficult problem.

The difference scheme used in this paper to deal with the discontinuity problems of the shock wave are valuable and worth generalization.

Key words one-dimensional unsteady, Harten solution, difference scheme

I. Introduction

The reflection problem of strong plane detonation wave is important and typical in the application of blow-up energy. This problem has been considered by many people. Prof. Huang Dun gives a series of analytical solutions for $t/k\times10^5<1.355$ in [2] and Wu Xiong-hua obtain the numerical solutions of the problem by using the separate singularity method in [3]. But because this problem appears companied with unsteady shock wave, boundary and initial values, and solutions with characteristic length, the results are either that the shock region is widened or that the wave peak is evened, or discontinued with the oscillation. So their results are not satisfactory.

In this paper, we use the 5-point difference scheme put forward by A. Harten in 1983 which was used to solve a kind of hyperbolic systems of conservation Laws and to computer the reflection problem of the strong plane detonation wave. We not only have tested the high accuracy of the Harten scheme, but also have showed the advantage of this method when it is applied to the strong plane detonation. The advantage is that it gets over the weakness of the discontinuity region width when we use the first-order scheme to computer, as well as the weakness of the discontinuity with the oscillation when we use the second-order to computer.

II. The Mathematical Model of the Problem

The one-dimensional unsteady movement equation of complete gas is

$$\left.\begin{aligned}&\frac{\partial u}{\partial t}+u\frac{\partial u}{\partial x}+\frac{1}{\rho}\frac{\partial p}{\partial x}=0\\&\frac{\partial \rho}{\partial t}+u\frac{\partial \rho}{\partial x}+\rho\frac{\partial u}{\partial x}=0\\&\frac{\partial p}{\partial t}+u\frac{\partial p}{\partial x}+\gamma_1\frac{\partial u}{\partial x}=0\end{aligned}\right\}\qquad(2.1)$$

γ is heat-insulation constant. Choose the coordinate system as the following Fig. 1. Neglecting the inner energy of the static air, then let $t=-t_1$ $(t_1>0)$ and there is a strong detonation on the plane at $x=R_0$. According to dimensional theory and equation (2.1), we know that before the detonation wave reaches the barrier $x=0$, the main parameters of the problem are total two dimensional independent constants except for γ and t. Thus the detonational incident wave $\widehat{AO}$ which propagates to the rigid solid barrier at $x=0$ has the auto-simulated property. When $t=0$, the incident wave meets the barrier without reflection, denoted as $\widehat{OB}$ $x=0$, $x=R_0$, $\widehat{AO}$ and $\widehat{OB}$ divide the plane x-t into three regions: in region I, there is auto-simulated solution; in region II there is an unsteady shock wave but average entropy and auto-simulated property; and region III is the static air before detonation.

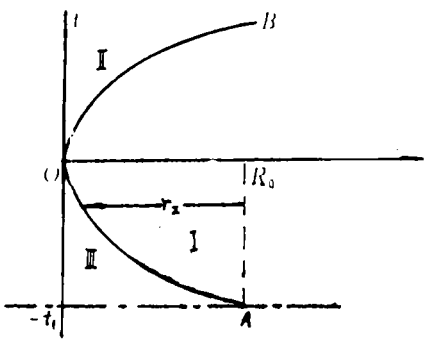

Fig. 1

For the convenience of the comparison and analysis of the computed results, we will use all constants appeared in [3] that is, $R_0=1$(m). $K=1$, $t_*=2.1718193\times10^{-5}\times K$ (s) and $E_0=1.077\times2.7349056\times10^{6}$ K(J/m^2) the released energy from the unit area.

III. The Summary of the Method and the Results of This Paper

The Harten scheme used in this paper is 5-point difference scheme which has second-order accuracy, and its convergence and stability have been considered in detail in [1], here we express the scheme as following without any proof:

$$v_j^{n+1}=v_j^n-\lambda(\bar f_{j+\frac12}^n-\bar f_{j-\frac12}^n)$$

$$\bar f_{j+\frac12}^n=\frac12[f(v_j)+f(v_{j+1})]+\frac{1}{2\lambda}\sum_{k=1}^{m}R_{j+\frac12}^k[\,g_j^k+g_{j+1}^k-Q^k(\nu_{j+\frac12}^k+r_{j+\frac12}^k)\,a_{j+\frac12}^k]$$

here:

$$\lambda=\frac{\Delta x}{\Delta t},\quad \nu_{j+\frac12}^k=\lambda a^k(v_{j+\frac12}),\quad a_{j+\frac12}^k=L_{j+\frac12}^k\,\Delta_{j+\frac12}v$$

$$\Delta_{j+\frac12}v=v_{j+1}-v_j$$

$$g_i^k=S_{i+\frac12}^k\max[0,\ \min(|\tilde g_{i+\frac12}^k|,\ \tilde g_{i-\frac12}^k\,S_{i+\frac12}^k)]$$

$$S_{i+\frac12}^k=\mathrm{sgn}(\tilde g_{i+\frac12}^k)$$

$$\bar{g}^k_{i+\frac{1}{2}}=0.5\,[Q^k(\nu^k_{i+\frac{1}{2}})-(\nu^k_{i+\frac{1}{2}})^2]\alpha^k_{i+\frac{1}{2}}$$

$$r^k_{i+\frac{1}{2}}=\begin{cases}(g^k_{i+1}-g^k_i)/\alpha^k_{i+\frac{1}{2}}, & \alpha^k_{i+\frac{1}{2}}\neq 0\\ 0, & \alpha^k_{i+\frac{1}{2}}=0\end{cases}$$

$$Q(x)=\begin{cases}x^2/4e+e, & |x|<2e\\ |x|, & |x|\geqslant 2e\end{cases}$$

$R[\cdot]$ denotes the right eigenvector obtained from matrix $[\cdot]$; a^k denotes the eigenvalue.

When we use the above scheme to compute the solution on every layer of the grids in II region, first we must know the right and left boundary value and the right and left sub-boundary value on the layer of the grids, and the initial conditions of the equation.

Firstly, we can know easily that, for the region II, the right boundary is determined by the solution of the region I. We have mentioned once above that the solution in the region I has the auto-simulated property. Here we first deduce the auto-simulated analytical solution in the region I by the dimensional theory in the mechanics.

When applying the Eular coordinate, the basic functions needed solving in (2.1) are the velocity u, density ρ and pressure p. By the Π theorem in the dimensional theory, there are follow:

$$u=\frac{r}{t}\mathscr{V};\qquad \rho=\rho_1\mathscr{R};\qquad p=\frac{\rho_1}{r^{-2}t^2}\mathscr{A} \tag{3.1}$$

here $\mathscr{V}$, $\mathscr{R}$, $\mathscr{A}$ are the variables without the dimension. ρ_1 is the density of the static air before the detonation.

When the strong detonational wave is produced by the air, the strong jump is generated within the flowings. The conservation of mass, momentum and energy should be satisfied when the gas passes the discontinuous surface. Denote one side of the discontinuous surface as the upper mark 1 and the other side as the under mark 2, then we have

$$\left.\begin{aligned}&\rho_1(u_1-c)=\rho_2(u_2-c)\\ &\rho_1(u_1-c)^2+p_1=\rho_2(u_2-c)+p_2\\ &\frac{1}{2}(u_1-c)^2+\frac{\gamma}{\gamma-1}\frac{p_1}{\rho_1}=\frac{1}{2}(u_2-c)^2+\frac{\gamma}{\gamma-1}\frac{p_2}{\rho_2}\end{aligned}\right\} \tag{3.2}$$

c is the velocity of the air-shock wave. In this case, the unique combination of the non-dimensional variables is $r^3t^{-2}/(E/\rho_1)$ according to the dimensional theory. This follows that the unique non-dimensional variable parameter is

$$\lambda=r/(E/\rho_1)^{1/3}\,t^{2/3} \tag{3.3}$$

to air-shock wave, coordinate r_2 is the function of time, so r_2 has dimension t, ρ_1 and E can not form the non-dimensional combination, we have:

$$r_2=(E/\rho_1)^{1/3}\,t^{2/3}\lambda^* \tag{3.4}$$

here λ^* is any a non-zero constant. Without lossing generality, let $\lambda^*=1$ then derivate (3.4) about time t:

$$c=\frac{2}{3}(E/\rho_1)^{1/3}t^{-1/3} \tag{3.5}$$

placing (3.5) into (3.2) and we notice that $u_1=0$ and $a_1/c=0$ on the air-shock wave (a_1 is the velocity of sound in the undisturbed medium), we have following on the air-shock wave:

$$\left.\begin{aligned} u_2 &= \frac{2}{\gamma+1}c = \frac{4}{3}\frac{1}{\gamma+1}\left(\frac{E}{\rho_1}\right)^{1/3} t^{-1/3} = \frac{4}{3}\frac{1}{\gamma+1}\left(\frac{E}{\rho_1}\right)^{1/2} r_2^{1/2} \\ \rho_2 &= \frac{\gamma+1}{\gamma-1}\rho_1 \\ p_2 &= \frac{2}{\gamma+1}\rho_1 c^2 = \frac{8}{9}\frac{\rho_1}{\gamma+1}\left(\frac{E}{\rho_1}\right)^{2/3} t^{-2/3} = \frac{8}{9}\frac{E}{\gamma+1} r_2 \end{aligned}\right\} \tag{3.6}$$

Compare (3.1) with the first equation of (3.6) and let new variable $\mathscr{Z} = \gamma\mathscr{A}/\mathscr{H}$

$$\left.\begin{aligned} &\frac{r}{r_2} = \lambda, \quad \frac{u}{u_2} = f = \frac{3}{4}(\gamma+1)\lambda\mathscr{V} \\ &\frac{\rho}{\rho_2} = g = \frac{\gamma-1}{\gamma+1}\mathscr{H}, \quad \frac{p}{p_2} = h = \frac{9}{8}\frac{\gamma+1}{\gamma}\lambda^2\mathscr{H}\mathscr{Z} \end{aligned}\right\} \tag{3.7}$$

We now can see that to solve r, ρ, u, p only need to compute the functions $\lambda(\mathscr{V})$, $\mathscr{Z}(\mathscr{V})$ and $\mathscr{H}(\mathscr{V})$. Placing (3.1) and (3.3) into (2.1) and replace with $\mathscr{Z} = v\mathscr{A}'/\mathscr{H}'$, derivate the first equation about $\mathscr{V}$, and derivate the second and the third equations after logarithm them, we have:

$$\left.\begin{aligned} \frac{d\mathscr{Z}}{d\mathscr{V}} &= \frac{\mathscr{Z}\{(\mathscr{V}+\gamma\mathscr{V}-2)(\mathscr{V}-\delta)^2-(\gamma-1)\mathscr{V}(\mathscr{V}-1)(\mathscr{V}-\delta)\} - [2(\mathscr{V}-1)+\mathscr{H}(\gamma-1)]\mathscr{Z}^2}{(\mathscr{V}-\delta)[\mathscr{V}(\mathscr{V}-1)(\mathscr{V}-\delta)+(\mathscr{H}-\mathscr{V})\mathscr{Z}]} \\ \frac{d\ln\lambda}{d\mathscr{V}} &= \frac{\mathscr{Z}-(\mathscr{V}-\delta)^2}{\mathscr{V}(\mathscr{V}-1)(\mathscr{V}-\delta)+(\mathscr{H}-\mathscr{V})\mathscr{Z}} \\ \frac{d\ln\mathscr{H}}{d\ln\lambda} &= \frac{1}{\mathscr{V}-\delta}\left(\delta-\mathscr{V}-\frac{(\mathscr{V}-1)\mathscr{V}(\mathscr{V}-\delta)+(\mathscr{H}-\mathscr{V})\mathscr{Z}}{\mathscr{Z}-(\mathscr{V}-\delta)^2}\right) \end{aligned}\right\} \tag{3.8}$$

in (3.8), $\delta = 2/3$, $\mathscr{H} = 2/3\gamma$. By applying the energy integral formular satisfied by the air-shock wave:

$$\lambda\left[\rho\mathscr{V} + \left(\mathscr{V}-\frac{2}{3}\right)\left(\frac{\mathscr{H}}{2}\mathscr{V}^2 + \frac{\mathscr{A}}{\gamma-1}\right)\right] = 0$$

repeat integral (3.8) then we obtain $\mathscr{Z}(\mathscr{V})$, $\lambda(\mathscr{V})$ and $\mathscr{H}(\mathscr{V})$. Placing $\mathscr{Z}(\mathscr{V})$, $\lambda(\mathscr{V})$ and $\mathscr{H}(\mathscr{V})$, (3.6) into (3.7) and we notice that: $\gamma < 7$; $\mathscr{V} \to 2/3\gamma$, thus we get the auto-simulated analysis solutions in region I:

$$t_1 = \left[R_0\left(\frac{E}{\rho_1}\right)^{1/3}\right]^{3/2}, \quad r_2 = \left(\frac{E}{\rho_1}\right)^{1/3}(t+t_1)^{2/3}, \quad \lambda(x,\ t) = \frac{R_0-x}{r_2}$$

$$\lambda = (1.8V)^{-2/3}[6(2.1V-1)]^{2/9}[3(1-1.2V)]^{-5/9}$$

$$-u = V - V_2 \times (1.8\lambda V)$$

$$\rho = \rho_2[6(2.1V-1)]^{5/9}\left[6\left(1-\frac{3}{2}V\right)\right]^{-10/3}[3(1-1.2V)]^{25/9}$$

$$p = p_2(1.8V)^{2/3}[6(1-1.5V)]^{-7/3}[3(1-1.2V)]^{5/3}$$

here V comes from the iteration of λ as following:

$$V^{(0)} = \frac{5\lambda^4+30}{63};$$

$$V^{(i+1)}=V^{(i)}+\frac{3}{2}\cdot\frac{\lambda-\lambda(V^{(i)})}{\lambda(V^{(i)})[1/(3V^{(i)}-10/7)-1/V^{(i)}+1/(1-1.2V^{(i)})]}$$

Now, we can compute the value of the right-boundary of region II.

Secondly, we can use the analysis solution in region I as the initial value of region II. But we must note that the original point is the singular point to the analysis solution and also the multiple-valued singular point. So we take the following two kinds of methods to avoid the singular point.

(1) Choosing an arbitrary $\Delta t>0$ and supposing Δt section as the initial compute time. Naturally this complicates the computation of the initial value and the key point of the complication is how to locate the shock wave on the Δt section. Now let us begin with $T=0.0$, and find the location of the grid points occupied by the shock wave (by using the method we have had, we can make certain the location table of the shock wave determined by Δt and go a step further to locate roughly the grid point location of the shock wave) and then deal these points with the weighted-average method. The new location computed from above can be considered as the more accurate location of the shock wave. For convenent comparison, we will use the table of the shock wave determined by Δt in [2] to locate the shock wave on some Δt sections. Once we have determined the location of the shock wave, we have determined initial value.

(2) Using the mirror-reflection method. Let us also begin with $T=0.0$, and add two nodes before the origin. Then we value these three points with the original first three node values respectively (notice that u needs to change its sign). Thus the shock wave seems to be passing through $x=0$ from the left of t-axis and reflecting to the right of t-axis, hence the singular point is avoided when we compute the initial value.

Thirdly, we will present the sub-boundary schemes. For the convenience of furture computation, we will not compute directly the u, p and ρ in (2.1), but the ρ , m and e in (2.1)', the equivalent equation system obtained by placing:

$$\begin{cases} u=m/\rho \\ p=(\gamma-1)(e-0.5\rho u^2) \end{cases}, \qquad W=\begin{pmatrix}\rho\\ m\\ e\end{pmatrix}$$

into (2.1)

$$\begin{pmatrix}\rho_t\\ m_t\\ e_t\end{pmatrix}+\begin{pmatrix} 0 & 1 & 0\\ \frac{\gamma-3}{2}\frac{m^2}{\rho^2} & (3-\gamma)\frac{m}{\rho} & \gamma-1\\ -\frac{\gamma me}{\rho^2}+(\gamma-1)\frac{m^3}{\rho^3} & \frac{\gamma e}{\rho}-\frac{3(\gamma-1)m^2}{2\rho^2} & \frac{\gamma m}{\rho}\end{pmatrix}\begin{pmatrix}\rho_x\\ m_x\\ e_x\end{pmatrix}=0 \qquad (2.1)'$$

(1) To the sub-boundary we can choose a general three-point explicit scheme:

$$v_j^{n+1}=v_j^n-\lambda\,(\bar f_{j+\frac12}^n-\bar f_{j-\frac12}^n)$$

$$\bar f_{j+\frac12}=\frac12\Big[f(v_j)+f(v_{j+1})-\frac{1}{\lambda}Q(\bar v_{j+\frac12})\,\Delta_{j+\frac12}v\Big]$$

$$\bar v_{j+\frac12}=\lambda a^k(v_{j+\frac12}),\qquad \Delta_{j+\frac12}v=v_{j+1}-v_j$$

$$Q(x)=\begin{cases} x/4\varepsilon+\varepsilon & |x|<2\varepsilon\\ |x| & |x|\geqslant 2\varepsilon\end{cases}$$

It is valuable to notice that this three point scheme is 1-order, and its combinational use with the 2-order scheme must lead to unsatisfactory computation results. So in the following we will give a sub-boundary difference scheme which has 2-order accuracy and be provided together with the 2-order Harten scheme.

(2) From a careful analysis of the Harten scheme, we can see that the key to the question is how to construct $g_1(-1,1,2)$. It is difficult to construct g_1 because of no definition of g_1 at the point -1. We are forced to remove the dependence of g_1 on the point -1 to that on the point $1(N+1)$ (see Fig. 2).

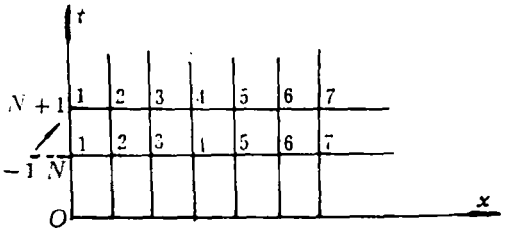

Fig. 2

When $x=0$ and $m=0$, we have $e_x=0$. Meanwhile, from $x=0$ we can also easily compute the three eigenvalues of the coefficient matrix $A(W)$ of W_x in the (2.1)': $a=(-c,\ 0,\ c)$ and 3×3 left characteristic matrix L. So:

$$a=(\Delta x\cdot L\cdot W_x)|_{x=0}=\Delta x\cdot\left(\frac{\rho_t}{2c},\ \rho_x,\ -\frac{\rho_t}{2c}\right)^T,\qquad c=\frac{\gamma p}{\rho}$$

hence:

$$v_1^1=-\lambda\cdot c,\quad v_1^2=0,\quad v_1^3=\lambda\cdot c$$

and

$$g_1=\begin{pmatrix}[Q(-\lambda c)-(-\lambda c)^2][(\rho_1^{n+1}-\rho_1^n)/4c]\lambda\\ 0\\ -[Q(\lambda c)-(\lambda c)^2][(\rho_1^{n+1}-\rho_1^n)/4c]\lambda\end{pmatrix}_{x=0}$$

Thus g_1 only relates to the physical quantities at the point $x=0$, hence it can apply the Harten scheme to the sub-outer layer. This has actually technically-improved the Harten scheme so that the Harten scheme can be used for the sub-outer layer and to increase the accuracy.

Lastly, we present the two schemes for the left boundary.

(1) First we give a left boundary differential scheme by taking the advantage of the characteristic relation. Suppose the three eigenvalues of the coefficient matrix of W_x are: $\lambda_1=u-c,\ \lambda_2=u,\ \lambda_3=u+c$. $u=0$ at the left boundary and so $\lambda_3=c>0$, that follows $m=0$, further more $e_x=0$, hence $e_1^{n+1}\approx e_3^{n+1}$. The second, suppose $(x_1,\ x_2,\ x_3)$ is the left eigenvector of $\lambda_2=u$, then: $(x_1,\ x_2,\ x_3)\ A(W)=u(x_1,\ x_2,\ x_3)$, expanding this formular and we notice that $u=0$, we have $x_1=-2\gamma e,\ x_2=0,\ x_3=2\rho$. With this eigenvector left multiplying the (2.1)' and expanded and simplified, we have:

$$\rho_1^{n+1}=\rho_1^n+\rho_1^n\cdot[(e_1^{n+1}-e_1^n)/\gamma e_1^n]$$

Thus, we have a group of solving differential schemes of left boundary:

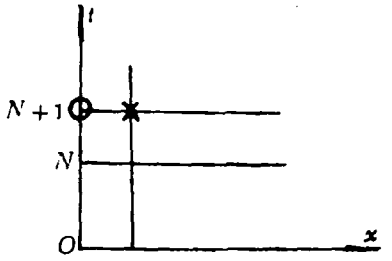

Fig. 3

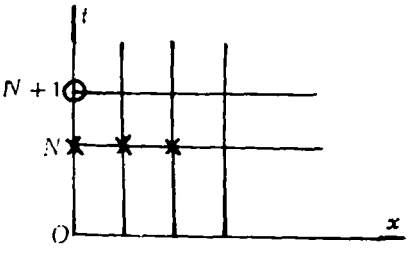

Fig. 4

$$m_1^{n+1}=0, \qquad e_1^{n+1}=e_1^n, \qquad \rho_1^{n+1}=\rho_1^n+\rho_1^n[(e_1^{n+1}-e_1^n)/\gamma e_1^n]$$

To the above formula, we know its order of convergence is $O(h+\tau)$ by its inference. So although the Harten scheme is two-order, when n is large enongh, a very little error of the boundary point will definitely affect the accuracy of the inner points. We must reconstruct a left boundary differential scheme by using the Taylor expansion so that its local order of convergence reaches two-order.

(2) Expansing e_1^{n+1} (Taylor expansion) at e_1^n. From $u=0$ and using the undetermined coefficient method and $m_0=0$, we can infer that:

$$e_1^{n+1}=e_1^n+\frac{\lambda}{2}\frac{\gamma e_1^n}{\rho_1^n}(m_1^n-4m_2^n)+\frac{\lambda^2}{2}\frac{\gamma e_1^n}{\rho_1^n}(\gamma-1)\left(e_1^n-2e_2^n+e_3^n+\frac{(m_2^n)^2}{\rho_1^n}\right)+O(\Delta t^3+\Delta x^2)$$

Then according to the entropy conservation equation:

$$\frac{\partial s}{\partial t}+u\cdot\frac{\partial s}{\partial x}=0$$

we know, on the solid barrier:

$$\left.\frac{\partial s}{\partial t}\right|_{x=0}=0$$

and once more, to the constant specific heat complete gas, we have:

$$\left.\frac{\partial}{\partial t}\left(\frac{p}{\rho^\gamma}\right)\right|_{x=0}=0$$

these follow that:

$$\rho_1^{n+1}=[e_1^{n+1}/e_1^n]^{1/\gamma}\cdot\rho_1^n$$

and we get a new left boundary schemes:

$$\begin{cases} m_1^{n+1}=0 \\ e_1^{n+1}=e_1^n+\dfrac{\lambda}{2}\dfrac{\gamma e_1^n}{\rho_1^n}(m_3^n-4m_2^n)+\dfrac{\lambda^2}{2}\dfrac{\gamma e_1^n}{\rho_1^n}(\gamma-1)\left(e_1^n-2e_2^n+e_3^n+\dfrac{(m_2^n)^2}{\rho_1^n}\right) \\ \rho_1^{n+1}=(e_1^{n+1}/e_1^n)^{1/\gamma}\rho_1^n \end{cases}$$

The above formula is two-order convergence and it is easily to see from the inference procedure.

IV. Numerical Results and Analysis

1. Combining the 1-order boundary, sub-boundary difference schemes and the Harten scheme with the first kind of method. Combining the 2-order boundary, sub-boundary difference schemes and the Harten scheme with the second kind of method. We have made a great deal of computation by using these two methods respectively, and made a comparison among the results of our computation and the results in [3] in the shock wave location, velocity density and pressure at the respectively same time. From the comparison we know the results in this paper have less

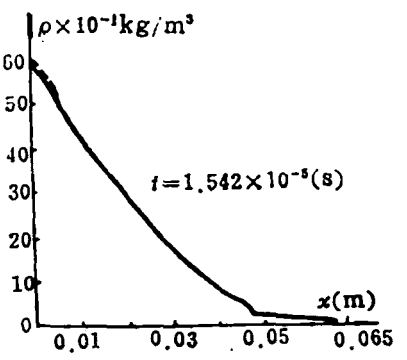

Fig. 5

errors than that in [3], and the errors of the results in this paper are usually from 0.2090% to 1.109%. In addition, the error of the shock wave location of the first kind method is larger than that of the second method and this result coincides with the result of the theoretical analysis. Fig. 5 shows the density image of $t=1.542\times10^{-5}$(s). The further analysis shows that the two kinds of methods have little difference at the shock wave, and the result is more satifatory than in [3].

2. Table 1 shows the analysis solutions and the numerical solutions of [3] and the two kinds of methods at time $t=1.00\times10^{-5}$ (s). In table 1 we can see that p_M and ρ_M but u_M computed from Harten scheme are better than that in [3]. However

Table 1 $T=1.00\times10^{-5}$(s) $T_0=0.20\times10^{-4}$(s)

Classes	Shock wave location	u_M(m/s)	ρ_M(kg/m³)	$p_M\times10^{-6}$(N/m²)
Numerical solution in [3]	0.021598	1606.0	2.3758	14.817
Numerical solution from the second kind method in this paper	0.021858	1599.5	2.4307	14.863
Numerical solution from the first kind method in this paper	0.021337	1596.3	2.4301	14.841
Analysis solution in this paper	0.021598	1606.8	2.5253	14.875

when we make the grid points more dense, we can also make the u_M better than in [3]. Besides, it is easy to see that the second method is closer to the analysis than the first method in this paper. In the same way, we compare the results of the period $t<1.05\times10^{-5}$ (s) and can obtain the satisfactory analogous conclusion.

3. In order to increase the accuracy of the computed results, we can use the mirror-reflection method to avoid the singular point which come from the computation with the beginning time $T_0=0.0$(s). Table 2 shows the results computated with the initial value $T_0=0.0$.(s) of the mirror-reflection method and the first kind method at $T=0.197\times10^{-5}$ (s).

Table 2 $T=0.197\times10^{-5}$(s) $T_0=0.0$(s) $\Delta x=4.9618\times10^{-4}$(m)

Variable	Classes	$J=1$	$J=2$	$J=3$	$J=4$	$J=5$	$J=6$	$J=7$	$J=8$	$J=9$
ρ_M (kg/m³)	*	18.181	18.067	17.795	17.337	16.362	14.266	7.8737	4.3427	4.1120
	**	24.431	23.723	20.413	16.682	9.2859	4.6881	4.3574	4.2323	4.1120
	***	6.2500	5.656	2.618	0.655	7.0761	9.5779	3.5163	0.1104	0.0000
$p_M\times10^{-6}$ (N/m²)	*	50.936	50.966	51.112	51.316	50.287	44.323	7.0418	7.0557	6.7165
	**	58.594	58.430	55.401	48.695	24.174	7.5034	6.9194	6.8160	6.7164
	***	7.6580	7.4640	4.289	2.621	26.113	36.8196	0.1224	0.2397	0.0001
u_M (m/s)	*	0.0000	75.156	157.36	244.76	286.62	176.32	−860.86	−2130.5	−2152.9
	**	0.0000	186.78	272.44	190.85	−724.91	−2129.3	−2184.7	−2168.7	−2152.9
	***	0.0000	111.62	115.08	53.91	1011.53	2305.62	1323.84	38.200	0.0000

* Mirror-reflection. ** The first kind method. *** Different value at the solid barrier.

In [4], it was mentioned that there is a vibration at the solid barrier when we use the mirror-reflection method, and the vibration smoothes the peak values of p, u and ρ. Table 2 shows how much of the peak value is erased. We will find that, when we compare a series of data of the same time, the vibrational and erasing phenomena will gradually disappear as time goes on. Table 3 shows the mirror-reflection method at $T=0.6\times10^{-5}$(s) and $T=0.197\times10^{-5}$(s).

Table 3 $T_0=0.0$(s) $\Delta x=4.9618\times10^{-4}$(m)

$t\times10^{-5}$(s)	Classes	Shock wave location	u_M(m/s)	ρ_M(kg/m³)	$p_M\times10^{-5}$(N/m²)	$p_0\times10^{-5}$(N/m²)
0.60	*	0.010420	975.15	5.8887	25.220	24.507
	**	0.010916	980.11	5.1233	25.067	24.424
0.197	*	0.0019847	272.44	20.413	55.401	58.596
	**	0.0029771	286.62	16.362	50.287	51.112

* Solution of the first kind method.

** Solution of the mirror-reflection method.

From Table 3 we know the error of the shock wave location of the mirror-reflection method is larger than that of the first kind method. But along with the time going on, the error is being reduced and when it reaches the points nearby the detonation point the error tends to zero. In Table 3, the shock wave deviates one node at $T=0.60\times10^{-5}$(s) and two nodes at $T=0.197\times10^{-5}$(s).

4. For the stability of the Harten scheme, [1] shows that the step of time must satisfy the condition:

$$\sigma=\max(|u|+c)\frac{\Delta t}{\Delta x}$$

For the accuracy of the Harten scheme, we can increase the number of the grid points so that Δx lessens and so does Δt. In this case, the time spent in computation increases at power of two to reach a certain time T. The Table 4 shows that the increase of the grid points obviously improves the accuracy. But on the other hand, in order to reach the time $T=0.30\times10^{-5}$(s) 131 nodes need only 15 layers while 200 nodes need 20 layers, hence the time spent in computation greatly increases. All above show that the Harten scheme is better than other former algorithms in dealing with the shock wave location and the numerical solution nearby the

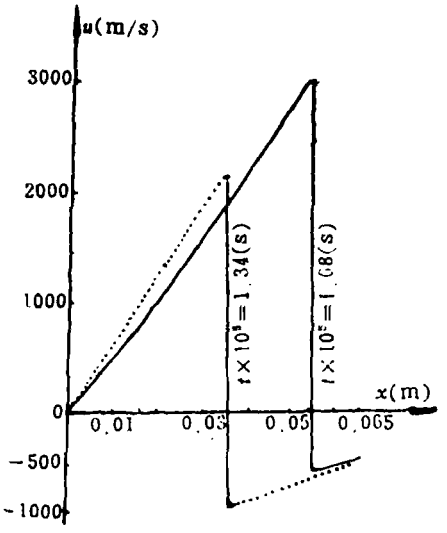

Fig. 6

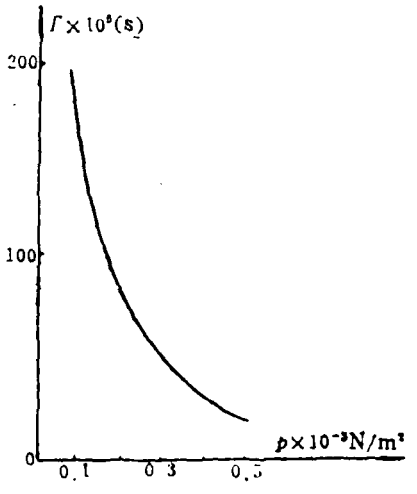

Fig. 7

Table 4 $T_0=0.20\times10^{-5}$(s) $T=0.30\times10^{-5}$(s)

Number of the nodes	Nmber of the grid layers	Shock wave location	u_M(m/s)	ρ_M(kg/m³)	$p_M\times10^{-6}$(N/m²)
131	15	0.0049618	470.38	11.265	40.159
200	20	0.0042250	446.46	11.766	39.516
Analysis solutions in [2]		0.0041000			

shock wave. Because of the more accurate data of the Harten scheme, it is an effective method in dealing with the problem of the discontinuity of the shock wave and is valuable to be generalized. The Fig. 5 to the Fig. 9 show some images in comparison with that in [3].

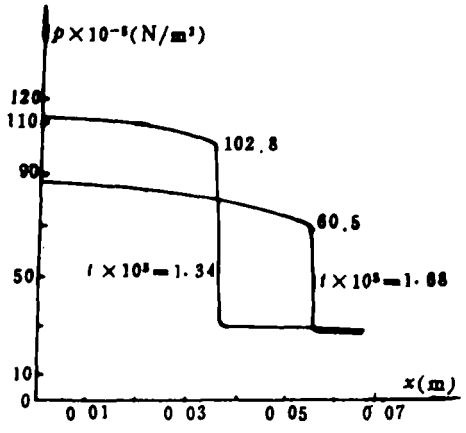

Fig. 8

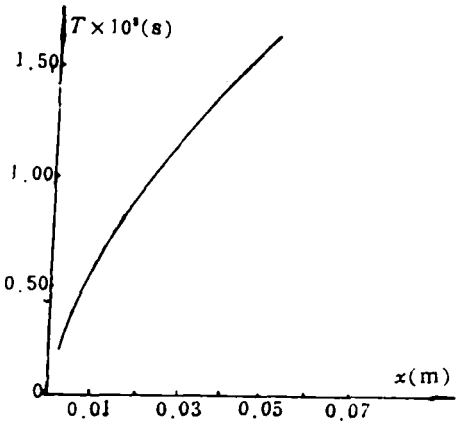

Fig. 9 The figure of the shock wave location (the second kind method)

Finally, the author sincerely thanks Wu Xiong-hua ph.D for his instruction in both theoretical inferenoe and problem analysis. The author also express my heartfelt gratitude to professor Li Shi-xong for his warmly guidance and help.

References

[1] Harten, A., *High Resolution Schemes for Hyperbolic Conservation*, Laus (1983).

[2] Huang Dun, A series of analytical solutions of higher order accuracy for air-dynamics coupled equations, *Yearly Thesis for Mathematics of Computation* (1979). (in Chinese)

[3] Wu Xiong-hua, The application of singularity-separation method to the computation of unsteady shock, *Mathematics of Computation and Computer Applications*, **3**, 3 (1982). (in Chinese)

[4] Zhon Ning, Reflection of unsteady blast wave computed by second order accurate MUDVL scheme, *Journal of Computational Physics Sinica*, **1**, 1 (1984), 21－30. (in Chinese)